Catalytic hydroarylation of ethylene using TpRu(L)(NCMe)Ph (L = 2,6,7-trioxa-1-phosphabicyclo[2,2,1]heptane): Comparison to TpRu(L′)(NCMe) Ph systems (L′ = CO, PMe 3, P(pyr) 3, or...

ARTICLE *in* ORGANOMETALLICS · OCTOBER 2012

Impact Factor: 4.13 · DOI: 10.1021/om300676e

6 AUTHORS, INCLUDING:

Claire McMullin
University of Bath
33 PUBLICATIONS **493** CITATIONS
SEE PROFILE

Michal Sabat
University of Virginia
405 PUBLICATIONS **7,891** CITATIONS
SEE PROFILE

ORGANOMETALLICS

Article

pubs.acs.org/Organometallics

Catalytic Hydroarylation of Ethylene Using TpRu(L)(NCMe)Ph (L = 2,6,7-Trioxa-1-phosphabicyclo[2,2,1]heptane): Comparison to TpRu(L′)(NCMe)Ph Systems (L′ = CO, PMe_3, $P(pyr)_3$, or $P(OCH_2)_3CEt$)

Evan E. Joslin,[†] Claire L. McMullin,[‡] T. Brent Gunnoe,*[,†] Thomas R. Cundari,*[,‡] Michal Sabat,[§] and William H. Myers[∥]

[†]Department of Chemistry, University of Virginia, Charlottesville, Virginia 22904, United States

[‡]Center for Advanced Scientific Computing and Modeling (CASCaM), University of North Texas, Denton, Texas 76203, United States

[§]Nanoscale Materials Characterization Facility, Department of Materials Science and Engineering, University of Virginia, Charlottesville, Virginia 22904, United States

[∥]Department of Chemistry, University of Richmond, Richmond, Virginia 23173, United States

Supporting Information

ABSTRACT: The Ru(II) complex TpRu[$P(OCH_2)_2(OCCH_3)$](NCMe)Ph (**4**; Tp = hydridotris(pyrazolyl)borate) has been synthesized and isolated. At 90 °C, TpRu[$P(OCH_2)_2OCCH_3$](NCMe)Ph in C_6D_6 produces TpRu[$P(OCH_2)_2(OCCH_3)$](NCMe)Ph-d_5 and C_6H_5D. TpRu[$P(OCH_2)_2(OCCH_3)$](NCMe)Ph catalyzes the hydrophenylation of ethylene at 90 °C to produce ethylbenzene with 90 turnovers (TOs) after 50 h. Catalyst deactivation occurs by the formation of the η^3-allyl complex TpRu[$P(OCH_2)_2(OCCH_3)$](η^3-C_3H_4Me). Kinetic studies of stoichiometric C_6D_6 activation by TpRu(L)(NCMe)Ph (L = CO, $P(OCH_2)_3CEt$, PMe_3 $P(OCH_2)_2(OCCH_3)$) to give TpRu(L)(NCMe)Ph-d_5 and C_6H_5D reveal that the reactions occur with the following relative rates: PMe_3 (k_{obs} = [1.36(4)] × 10^{-5} s^{-1}) > $P(OCH_2)_3CEt$ (k_{obs} = 1.20(2) × 10^{-5} s^{-1}) > $P(OCH_2)_2(OCCH_3)$ (k_{obs} = 7.2(5) × 10^{-6} s^{-1}) > CO (k_{obs} = [4.62(3)] × 10^{-6} s^{-1}). These rates correlate linearly with Ru(III/II) potentials of the four TpRu(L)(NCMe)Ph complexes. DFT calculations have been used to model catalytic olefin hydroarylation by TpRu[$P(OCH_2)_2(OCCH_3)$](NCMe)Ph (**4**) and to rationalize the observed differences in the various TpRu(L)(NCMe)Ph catalysts.

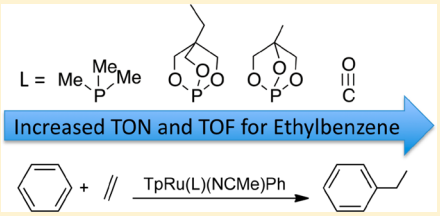

INTRODUCTION

Reported examples of catalytic metal-mediated C−H functionalization of aromatic substrates have increased substantially in recent years.[1−12] The use of transition-metal catalysts for the addition of aromatic C−H bonds across C═C bonds of olefins (i.e., olefin hydroarylation) is an area of increasing interest (eq 1).[1,2,9−11,13−16] Friedel−Crafts catalysts, typically a combination

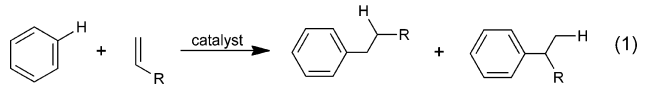

(1)

of a main-group Lewis acid with a Brønsted acid, can be used for aromatic alkylation,[17−24] but transition-metal catalysts that function by a pathway that incorporates olefin insertion into a metal−aryl bond and metal-mediated C−H activation offer potential advantages over Friedel−Crafts-catalyzed reactions (Scheme 1).[13,25,26] Examples of transition-metal catalysts for olefin hydroarylation using substrates that are functionalized with heteroatomic groups or halogens are known,[9,11,15,27−31] but examples of catalysts that convert hydrocarbons (e.g., benzene, ethylene, or propene) are relatively rare.[13,32−35] The production of alkylarenes is a large-scale business for the petrochemical industry.[17,18,20,24] For example, in the United States >15 million tons of ethylbenzene are produced annually.[19]

Scheme 1. Prototypical Catalytic Cycle for Ethylene Hydroarylation That Incorporates Metal-Mediated C−H Activation

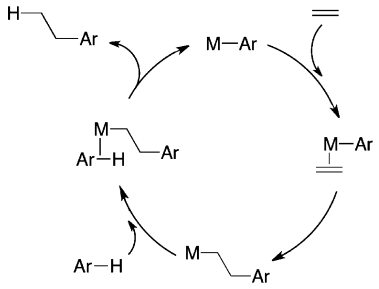

Received: July 19, 2012
Published: September 24, 2012

   dx.doi.org/10.1021/om300676e | *Organometallics* 2012, 31, 6851−6860

Chart 1. Competition between Ethylene Insertion into the Ru−Ph Bond and Ethylene C−H Activation

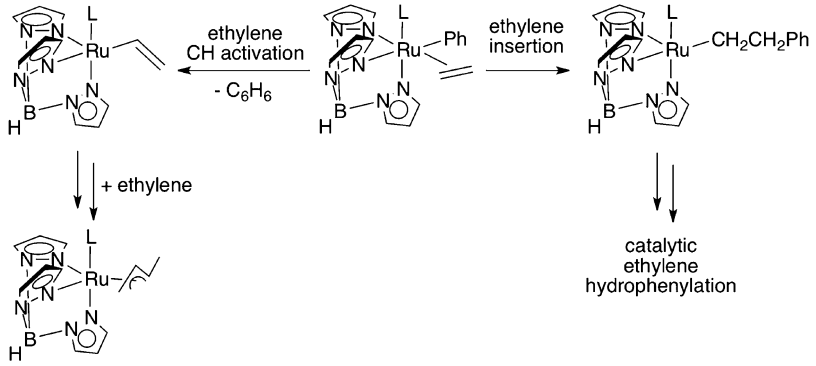

Transition-metal catalysts for olefin hydroarylation of hydrocarbons include ruthenium, iridium, and platinum complexes.[10,13,16,25,26,28,32−34,36−41] Previously, our groups have investigated complexes of the form TpRu(L)(NCMe)Ph (Tp = hydridotris(pyrazolyl)borate; L = CO, PMe_3, $P(pyr)_3$, $P(OCH_2)_3CEt$; pyr = *N*-pyrrolyl) for the catalytic hydroarylation of olefins.[13,25,35,42−47] Since the initial report of catalysis with TpRu(CO)(NCMe)Ph,[46] we have used the TpRu(L)(NCMe)Ph motif to probe structure/activity relationships through variation of the ligand L.[25,42−44] A central issue for successful catalysis is the relative rate of ethylene insertion versus ethylene C−H activation from TpRu(L)(η^2-C_2H_4)Ph intermediates (Chart 1).[25] For example, the catalyst with L = PMe_3 was found to activate benzene ∼3 times more rapidly than TpRu(CO)(NCMe)Ph; however, catalytic ethylene hydrophenylation by TpRu(PMe_3)(NCMe)Ph was inhibited by slow ethylene insertion, which results in competitive ethylene C−H activation.[44] The complex with L = $P(pyr)_3$ is too sterically bulky for ethylene coordination.[43] The bicyclic phosphite complex TpRu[$P(OCH_2)_3CEt$](NCMe)Ph provided an active catalyst for ethylene hydrophenylation, but ethylene C−H activation competes with ethylene insertion and ultimately results in catalyst deactivation.[42] On the basis of these results, we sought a ligand with a steric profile similar to that of $P(OCH_2)_3CEt$ but with less electron donating ability. Herein, we disclose the synthesis and studies of catalytic olefin hydroarylation using TpRu[$P(OCH_2)_2(OCCH_3)$](NCMe)Ph.

Scheme 2. Synthesis of TpRu[$P(OCH_2)_2(OCCH_3)$](NCMe)Ph (4)[a]

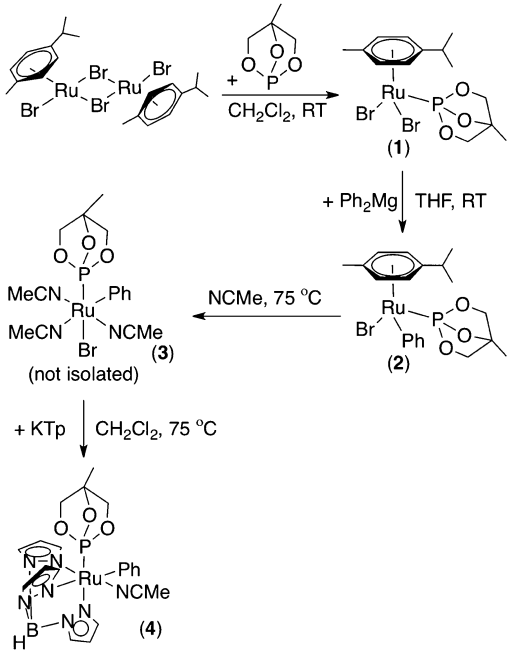

[a]RT = room temperature.

RESULTS AND DISCUSSION

Synthesis of TpRu[$P(OCH_2)_2(OCCH_3)$](NCMe)Ph. We have reported the preparation of (η^6-C_6H_6)Ru(L)Cl_2 (L = PPh_3 $P(OMe)_3$, PMe_3, $P(OCH_2)_3CEt$, CO, $P(OCH_2)_2(OCCH_3)$) and (η^6-*p*-cymene)Ru(L)Cl_2 (L = $P(OCH_2)_3CEt$, $P(OCH_2)_2(OCCH_3)$, $P(OMe)_3$, PPh_3) and data which indicate that $P(OCH_2)_2(OCCH_3)$ is less donating than the other P-based ligands studied.[48] We have now prepared (η^6-*p*-cymene)Ru[$P(OCH_2)_2(OCCH_3)$]Br_2 (**1**) by a similar route (Scheme 2). Stirring [(η^6-*p*-cymene)Ru(Br)(μ-Br]$_2$ and $P(OCH_2)_2(OCCH_3)$ in CH_2Cl_2 leads to the formation of complex **1** in 91% isolated yield. The ^{31}P NMR spectrum of **1** shows a resonance at 140 ppm for the $P(OCH_2)_2(OCCH_3)$ ligand. Stirring **1** and 1 equiv of $Ph_2Mg(THF)_2$ at room temperature gives the phenylated species (η^6-*p*-cymene)Ru[$P(OCH_2)_2(OCCH_3)$](Ph)Br (**2**). The formation of **2** is evident by the ^{31}P NMR spectrum, which shows a downfield shift (155.5 ppm) of ∼15 ppm relative to **1**. The *p*-cymene ligand can be displaced upon heating at 75 °C for 4 h in NCMe to yield the putative complex $(NCMe)_3Ru[P(OCH_2)_2(OCCH_3)](Ph)Br$ (**3**), which has not been isolated or characterized beyond in situ ^1H NMR spectroscopy.[49] Heating complex **3** and KTp in CH_2Cl_2 for 4 h at 75 °C produces TpRu[$P(OCH_2)_2(OCCH_3)$](NCMe)Ph (**4**) in 44% isolated yield. The ^1H NMR spectrum of **4** is consistent with an asymmetric complex. Cyclic voltammetry of complex **4** in NCMe shows a reversible redox couple at $E_{1/2}$ = 0.69 V (vs NHE).

A single crystal of **4** suitable for X-ray structure determination was obtained from slow evaporation of a CH_2Cl_2/pentane (∼1/1 v/v) solution at room temperature; the resulting solid-state structure is shown in Figure 1, and crystallographic data are given in Table 1. The phosphite has two smaller O−P−O angles of 93.76(1) and 93.56(1)° and one larger angle at 100.27(2)°. The P−O bond for the arm of the phosphite without a CH_2 is slightly longer at 1.643(2) Å versus 1.628(2) and 1.6290(2) Å.

dx.doi.org/10.1021/om300676e | *Organometallics* 2012, 31, 6851−6860

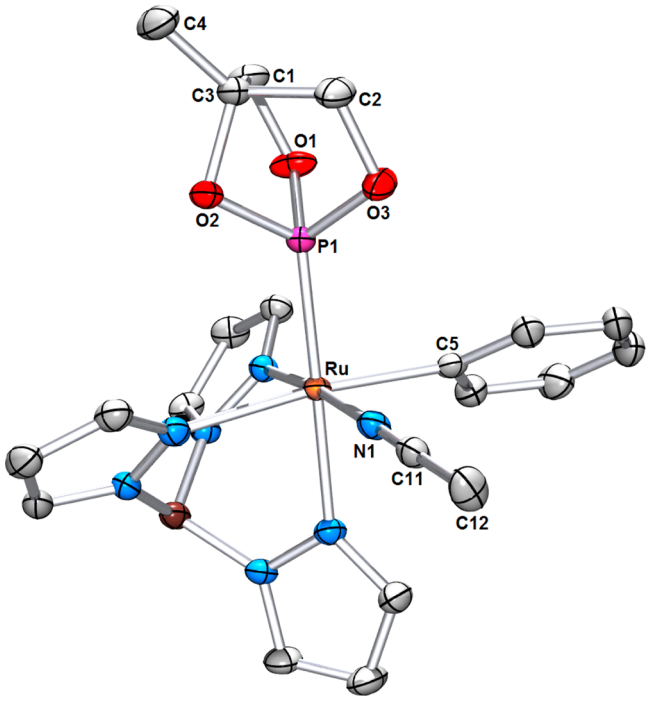

Figure 1. ORTEP of TpRu[$P(OCH_2)_2(OCCH_3)$](NCMe)Ph (**4**) (50% probability, hydrogen atoms omitted for clarity). Selected bond lengths (Å): Ru−N1, 2.009(2); Ru−C5, 2.092(2); N1−C11, 1.147(2); C11−C12, 1.445(4); Ru−P1, 2.1602(6); P1−O1, 1.628(2); P1−O2, 1.643(2); P1−O3, 1.629(2). Selected bond angles (deg): N1−Ru−C5, 88.55(9); N1−Ru−P1, 92.58(6); C5−Ru−P1, 92.83(6); N1−C11−C12, 178.1(3); O3−P1−O1, 100.27(2); O3−P1−O2, 93.76(1); O1−P1−O2, 93.56(1); O1−P1−Ru, 119.21(7); O3−P1−Ru, 120.47(7); C1−O1−P1, 108.52(2); C3−O2−P1, 98.56(1); C2−O3−P1, 107.95(2).

Table 1. Selected Crystallographic Data for TpRu[$P(OCH_2)_2(OCCH_3)$](NCMe)Ph·CH_2Cl_2

empirical formula	$C_{22}H_{27}BCl_2N_7O_3PRu$
fw	8651.26
cryst syst	triclinic
space group	$P\bar{1}$
a, Å	7.8849(2)
b, Å	12.4914(3)
c, Å	14.3261(3)
α, deg	81.278(1)
β, deg	88.846(1)
γ, deg	75.726(1)
V, Å^3	1351.43(6)
Z	2
D_{calcd}, Mg/m^3	1.600
cryst size (mm)	0.42 × 0.19 × 0.08
R1, wR2 ($I > 2(I)$)	0.0386, 0.1110
GOF	0.898

The C−O−P bond angle is approximately 10° less for the portion of the phosphite lacking the CH_2, whereas the other C−O−P angles are 108.52(2) and 107.95(2)°.

Stoichiometric Benzene Activation. On the basis of mechanistic studies, we have suggested that benzene C−H activation by TpRu(L)(NCMe)Ph (L = CO, PMe_3, $P(OCH_2)_3CEt$) complexes most likely involves dissociation of NCMe, which gives an open coordination site for C_6D_6 coordination, followed by C−D activation.[35,42,44,45] Complex **4** undergoes the same reaction (eq 2), and similar to the case for the previously reported

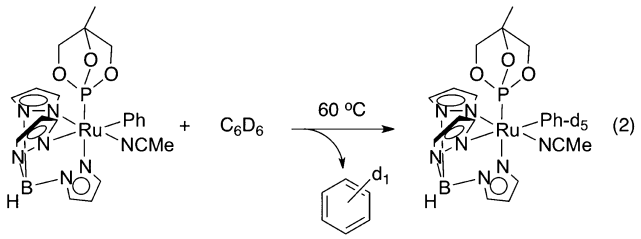

TpRu(L)(NCMe)Ph complexes, the addition of NCMe is necessary to inhibit decomposition and allow the C−D activation to proceed in quantitative yield (^{1}H NMR spectroscopy).[44] For example, monitoring a solution of **4** in C_6D_6 at 60 °C by ^{1}H NMR spectroscopy reveals the formation of benzene (C_6H_5D) and the disappearance of resonances for the phenyl ligand of **4**. These observations are consistent with C−D activation of C_6D_6 by complex **4**; however, partial decomposition of **4** also occurs. The addition of 1 equiv of NCMe to the solution results in clean conversion of **4** to **4**-d_5 with >90% yield (by ^{1}H NMR spectroscopy).[50] In order to compare C_6D_6 activation by complex **4** to other TpRu(L)(NCMe)Ph complexes, the rate of reaction with C_6D_6 was determined. A k_{obs} value of $[7.2(5)] \times 10^{-6}$ s^{-1} (60 °C) was found by fitting the plot concentration of perprotio-**4** versus time to a first-order decay (Figure 2). The k_{obs} values for C_6D_6

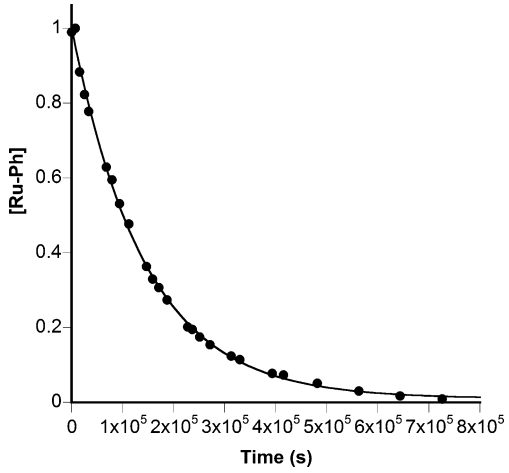

Figure 2. Representative plot of C−D activation of C_6D_6 by TpRu-[$P(OCH_2)_2(OCCH_3)$](NCMe)Ph (**4**) in C_6D_6 at 60 °C monitored by ^{1}H NMR spectroscopy ($k_{obs} = [7.0(2)] \times 10^{-6}$ s^{-1}, $R^2 = 0.99$). The plot shows the relative amount of protio-phenyl ligand (integrated against an internal standard) of **4** as a function of time.

activation by TpRu(L)(NCMe)Ph (L = CO, PMe_3, $P(pyr)_3$, $P(OCH_2)_3CEt$) have been previously determined,[25] and a plot of k_{obs} for C_6D_6 activation vs Ru(III/II) redox potential reveals a clear trend (Table 2, Figure 3). The rate of C_6D_6 activation decreases as the Ru(III/II) potential becomes more positive. The slowest C_6D_6 activation occurs with TpRu(CO)(NCMe)Ph with $k_{obs} = [4.62(3)] \times 10^{-6}$ s^{-1}, whereas the most electron-rich metal center, TpRu(PMe_3)(NCMe)Ph, exhibits the fastest rate of C_6D_6 activation with $k_{obs} = [1.36(4)] \times 10^{-5}$ s^{-1} (Table 2). The plot of $E_{1/2}$ vs k_{obs} gives a linear correlation with an R^2 value of 0.92 and a slope of −1.29 s^{-1} V^{-1} (Figure 3).

dx.doi.org/10.1021/om300676e | *Organometallics* 2012, 31, 6851−6860

Table 2. Ru(III/II) Potentials and Rate Constants for the Activation of C_6D_6 at 60 °C by TpRu(L)(NCMe)Ph[a]

L	Ru(III/II) potential (V vs NHE)	k_{obs} ($\times 10^{-5}$ s^{-1})[a]	rel k_{obs}
PMe_3	0.29	1.36(4)	3.0
$P(OCH_2)_3CEt$	0.54	1.20(2)	2.6
$P(OCH_2)_2(OCCH_3)$	0.69	0.72(5)	1.6
CO	1.03	0.462(3)	1

[a]0.065 mmol of NCMe.

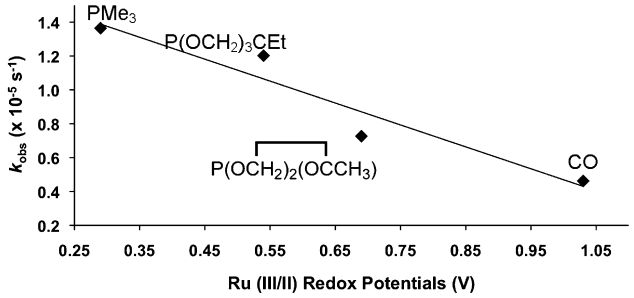

Figure 3. Linear fit for plot of k_{obs} ($\times 10^{-5}$ s^{-1}) values vs Ru(III/II) potentials (vs NHE, V) for the C−D activation of C_6D_6 by TpRu(L)(NCMe)Ph at 60 °C with 0.065 mmol of added NCMe (R^2 = 0.92, m = −1.29 s^{-1} V^{-1}).

Catalytic Hydrophenylation of Ethylene by TpRu[P-(OCH$_2$)$_2$(OCCH$_3$)](NCMe)Ph. Scheme 3 shows the proposed catalytic cycle for ethylene hydrophenylation by TpRu(L)-(NCMe)Ph complexes.[25,35,42−44] Through experimental and computational mechanistic studies, it has been concluded that the active catalytic species is generated from TpRu(L)(NCMe)-Ph by dissociation of NCMe. Subsequent coordination of ethylene to Ru followed by olefin insertion into the Ru−Ph bond yields TpRu(L)(CH_2CH_2Ph).[35] Benzene coordination and C−H activation releases ethylbenzene and regenerates the active catalyst (Scheme 3).[25,42] The catalyst resting state has been identified as TpRu(L)(η^2-C_2H_4)(CH_2CH_2Ph),[25] and the rate-limiting step of the catalytic cycle is the aromatic C−H bond activation event.

Complex **4** catalyzes the hydrophenylation of ethylene. At 90 °C, using 0.025 mol % (relative to benzene) of **4** with 15 psi of ethylene results in 90 turnovers (TOs) of ethylbenzene after 50 h. Similar to previously reported Ru(II) complexes,[25] the catalyst activity is inversely proportional to ethylene concentration (Figure 4). For example, at 90 °C after 8 h, the TOs were

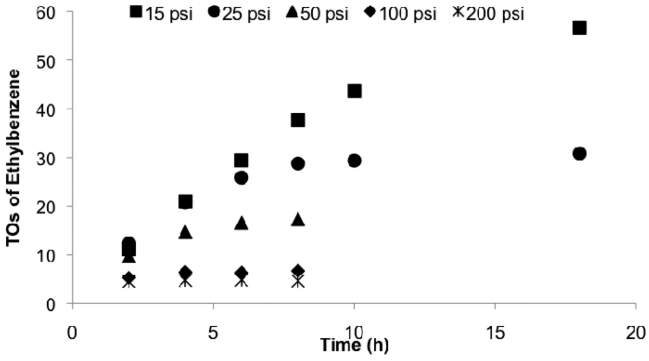

Figure 4. Comparison of catalytic hydrophenylation of ethylene by complex **4** (90 °C) at variable ethylene pressures.

38 (15 psi), 29 (25 psi), 17 (50 psi), 7 (100 psi) and 5 (200 psi). The optimal conditions for catalysis are at 90 °C with 15 psi of ethylene. Under most conditions, no diethylbenzene or styrene is detected.

Increasing the temperature (75, 90, and 105 °C) at 15 psi of ethylene increases the rate of ethylbenzene production (Figure 5). During the first 4 h of catalysis the slope is linear (i.e., no evidence of catalyst deactiation is observed). Therefore, initial TOF values were calculated at 4 h: TOF = 2.1×10^{-4} s^{-1} at 75 °C, 1.5×10^{-3} s^{-1} at 90 °C, and 3.5×10^{-3} s^{-1} at 105 °C. In comparison, the TOF using TpRu(CO)(NCMe)Ph (90 °C, calculated after 4 h of

Scheme 3. Proposed Catalytic Cycle for the Hydrophenylation of Ethylene using TpRu(L)(NCMe)$_3$Ph (L = CO, P(OCH$_2$)$_3$CEt, P(OCH$_2$)$_2$(OCCH$_3$))

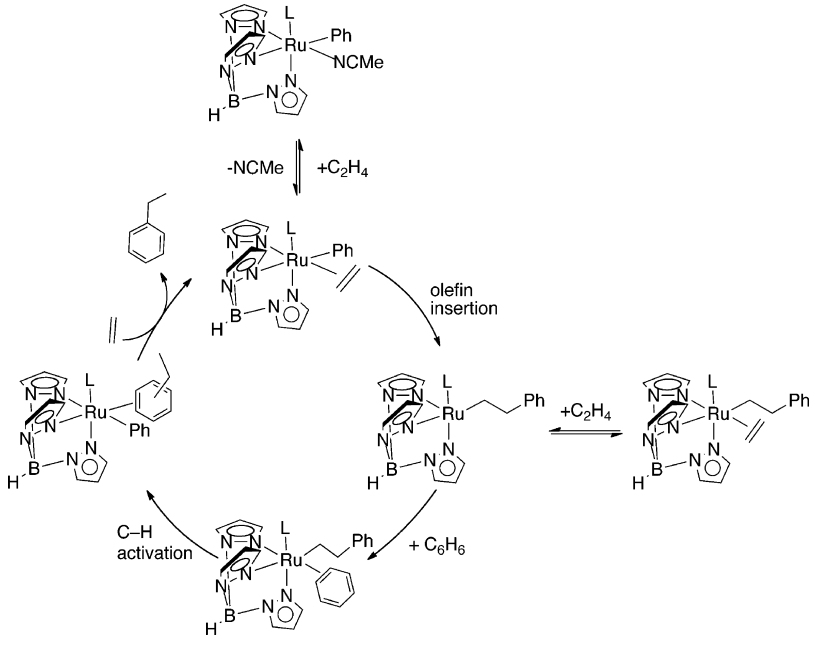

dx.doi.org/10.1021/om300676e | Organometallics 2012, 31, 6851−6860

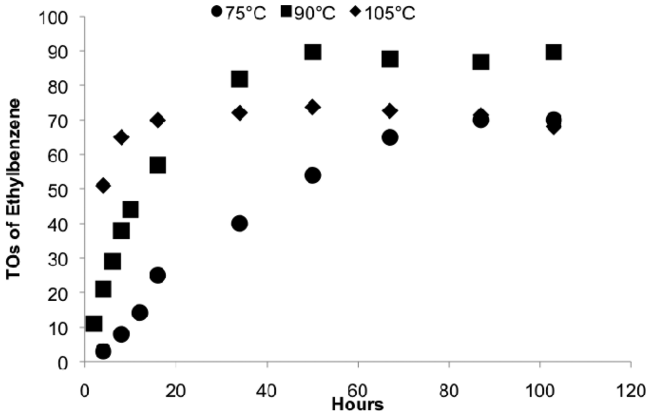

Figure 5. Comparison of catalytic hydrophenylation of ethylene by complex **4** at 15 psi of ethylene and variable temperature.

catalysis) is 6.7×10^{-3} s^{-1} (note that this TOF and the turnover number (TON) are different from previously published data[35] as a result of different conditions). Thus, at 90 °C and 15 psi of ethylene TpRu[P(OCH$_2$)$_2$(OCCH$_3$)](NCMe)Ph is a less active catalyst than TpRu(CO)(NCMe)Ph by a factor of ~4.5.

^{1}H NMR spectroscopy of the nonvolatiles after catalyst deactivation indicates that the product of catalyst deactivation is the η^3-allyl complex TpRu[P(OCH$_2$)$_2$(OCCH$_3$)](η^3-C$_3$H$_4$Me) (**5**). Complex **5** has been isolated and characterized by ^{1}H NMR spectroscopy and mass spectrometry (eq 3). The ^{1}H NMR spectrum reveals minor impurities that we were not able to

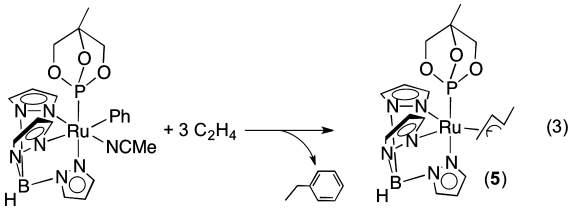

remove (see the Supporting Information). GC-MS analysis of **5** shows the expected parent peak for complex **5** in addition to peaks for complexes with an additional 1 and 2 equiv of ethylene. Thus, we speculate that the minor impurities are allyl complexes with propyl and pentyl groups that result from insertion of an additional 1 or 2 equiv of ethylene (see the Supporting Information). The deactivation of **4** under catalytic conditions is identical with that observed for TpRu(PMe$_3$)(NCMe)Ph and TpRu[P(OCH$_2$)$_3$CEt](NCMe)Ph.[42,44] It has been shown previously that the allyl complex is formed due to an electron-rich Ru center, which results in vinyl C–H activation competing with ethylene insertion.[25] This ultimately leads to the formation of an η^3-allyl species due to the formation of a Ru–vinyl species followed by olefin insertion and isomerization.

Catalytic Hydroarylation by TpRu[P(OCH$_2$)$_2$(OCCH$_3$)](NCMe)Ph (4) using Ethylbenzene and Ethylene. Regioselective production of dialkylbenzenes is a challenging reaction. Friedel–Crafts catalysts generally give a mixture of 1,2-, 1,3-, and 1,4-dialkylbenzenes.[17] To determine if complex **4** exhibits selectivity for the production of diethylbenzenes, ethylene hydroarylation studies were performed using ethylbenzene. Upon the reaction of ethylbenzene and ethylene at 90 °C and 15 psi of ethylene with 0.025 mol % of **4**, a 2/1 ratio of 1,3- to 1,4-diethylbenzene (8 and 4 TOs after 4 h, respectively) was observed (eq 4). No evidence for the formation of 1,2-diethylbenzene was obtained. In the case of TpRu(CO)-

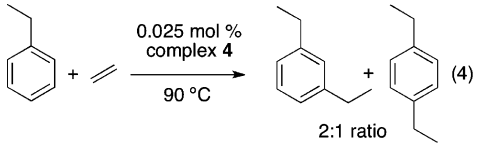

(NCMe)Ph, the same 2/1 ratio of 1,3-diethylbenzene to 1,4-diethylbenzene is observed.[35] The TOF for the formation of diethylbenzene after 4 h is 8.3×10^{-4} s^{-1}, which is 1.8 times slower than the formation of ethylbenzene from benzene and ethylene (see above). With Friedel–Crafts catalysts, ethylbenzene is generally more reactive than benzene, which renders selective monoalkylation challenging.[25]

Attempted Hydrophenylation of Monosubstituted Olefins. Hydrophenylation of 1-pentene (160 equiv relative to **4**) was attempted. Only minimal production of 2-phenylpentane (~0.3 TOs) was observed after 8 h. Increasing the amount of 1-pentene did not give increased production of phenylpentane. Additionally, catalytic hydrophenylation was unsuccessful with the substrates methyl acrylate, methyl vinyl ketone, and propylene (at pressures from 25 to 150 psi and temperatures of 90 or 110 °C).

DFT Calculations of Ethylene Hydrophenylation by TpRu[P(OCH$_2$)$_2$(OCCH$_3$)](NCMe)Ph. Density functional theory (DFT) calculations were used to probe the conversion of TpRu[P(OCH$_2$)$_2$(OCCH$_3$)](NCMe)Ph (**4**) and ethylene to ethylbenzene (Scheme 4). Comparison of the free energy surface for L = P(OCH$_2$)$_2$(OCCH$_3$) with that previously reported for PMe$_3$, P(pyr)$_3$, P(OCH$_2$)$_3$CEt, and CO shows little variation in the overall shape and energies of the intermediates and transition states for ethylene insertion (**TS1**; Scheme 4) and benzene C–H activation (**TS2**; Scheme 4).[25] As seen for other π-acidic ligands (e.g., P(OCH$_2$)$_3$CEt and CO), the coordination mode of benzene in TpRu(L)(benzene)(CH$_2$CH$_2$Ph) (**E** in Scheme 4) is η^2-C=C, while for less π-acidic ligands an η^2-C–H coordination mode of benzene was calculated to be the most favorable.[25] There is very little difference in calculated energetics starting from complex **4** in comparison to identical calculations for TpRu[P(OCH$_2$)$_3$CEt](NCMe)Ph.[42] In fact, calculated energies for the two phosphites differ by only ~1 kcal/mol, which is within the error of these calculations.

Comparison of TpRu(L)(NCMe)Ph Catalysts. On the basis of Ru(III/II) potentials (see Table 2), the relative Ru-based electron densities of the complexes TpRu(L)(NCMe)Ph can be assigned as L = PMe$_3$ > P(OCH$_2$)$_3$CEt > P(OCH$_2$)$_2$(OCCH$_3$) > P(pyr)$_3$ > CO. Table 3 provides a comparison of the results from hydrophenylation of ethylene using TpRu(L)(NCMe)Ph complexes.

For the three complexes TpRu(L)(NCMe)Ph (L = P(OCH$_2$)$_3$CEt, P(OCH$_2$)$_2$(OCCH$_3$), CO) that serve as catalysts for the hydrophenylation of ethylene, the catalyst activity and longevity vary as a function of the identity of L. The observed trends in TON and TOF for TpRu(L)(NCMe)Ph catalysts are inverse to the trend in relative rates of benzene activation by TpRu(L)(NCMe)Ph. Our studies provide a clear rationalization for the trends in TON. For TpRu(L)(NCMe)Ph complexes (L = P(OCH$_2$)$_3$CEt, P(OCH$_2$)$_2$(OCCH$_3$), CO, PMe$_3$), a primary factor in the longevity of the catalyst is the relative rate of olefin

dx.doi.org/10.1021/om300676e | Organometallics 2012, 31, 6851–6860

Scheme 4. Calculated Gibbs Free Energies (kcal/mol) for Hydrophenylation of Ethylene by TpRu[P(OCH$_2$)$_2$(OCCH$_3$)](NCMe)Ph

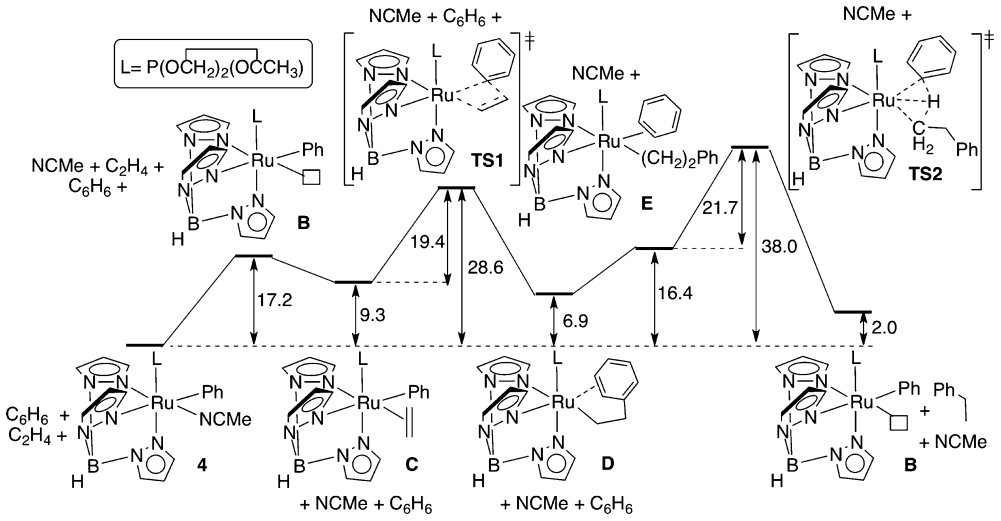

Table 3. Comparison of TON and TOF for Ethylbenzene Production from Catalytic Hydrophenylation of Ethylene by TpRu(L)(NCMe)Ph Complexes

L	TON	time (h)	TOF (s^{-1})[c]	rel TOF	$E_{1/2}$ (V vs NHE)
CO	415[a]	40	6.7×10^{-3}	14	1.03
P(pyr)$_3$	0				0.76
P(OCH$_2$)$_2$(OCCH$_3$)	90[b]	50	1.5×10^{-3}	3	0.69
P(OCH$_2$)$_3$CEt	20[b]	24	4.8×10^{-4}	1	0.54
PMe$_3$	0[b]				0.29

[a]Products from catalyst decomposition are unknown, but under most conditions TpRu(CO)(η^3-C$_3$H$_4$Me) is not formed. [b]Catalyst deactivation occurs by formation of TpRu(L)(η^3-C$_3$H$_4$Me). [c]Calculated after 4 h at 90 °C with 15 psi of ethylene and 0.025 mol % of catalyst.

insertion versus olefin C−H activation. As previously reported and confirmed again here by our analysis of P(OCH$_2$)$_2$(OCCH$_3$), altering the donor ability of L has a relatively minor impact on the $\Delta G^{\ddagger}$ values for benzene and ethylene C−H activation.[25] However, the identity of L has a substantial impact on the activation barrier for ethylene insertion into the Ru−Ph bond of TpRu(L)(η^2-C$_2$H$_4$)Ph complexes. With one exception, TpRu[P(pyr)$_3$](NCMe)Ph,[25] increased donor ability of L results in an increase in the calculated $\Delta G^{\ddagger}$ for olefin insertion from TpRu(L)(η^2-C$_2$H$_4$)Ph complexes, which results in competition between ethylene C−H activation and ethylene insertion into the Ru−Ph bond. In the presence of excess ethylene, the C−H activation of ethylene by TpRu(L)(η^2-C$_2$H$_4$)Ph results in the formation of η^3-allyl complexes TpRu(L)(η^3-C$_3$H$_4$Me) (allyl complexes have been isolated for L = CO, PMe$_3$, P(OCH$_2$)$_3$CEt, P(OCH$_2$)$_2$(OCCH$_3$)).[25] Table 4 shows the calculated $\Delta G^{\ddagger}$ values for ethylene insertion from TpRu(L)(η^2-C$_2$H$_4$)Ph complexes with $\Delta\Delta G^{\ddagger}$ = ~6.2 kcal/mol. The calculated $\Delta\Delta G^{\ddagger}$ for ethylene insertion is much larger than the $\Delta\Delta G^{\ddagger}$ for benzene C−H activation as the ligand L is varied. For TpRu(PMe$_3$)(NCMe)Ph, ethylene insertion does not compete with ethylene C−H activation, and catalytic production of ethylbenzene is not observed.[45] For TpRu[P(OCH$_2$)$_3$CEt](NCMe)Ph, ethylene insertion is more rapid than ethylene C−H activation, but the

Table 4. Calculated $\Delta G^{\ddagger}_{\text{insertion}}$ (kcal/mol) for Olefin Insertion (TS1, Scheme 4) for TpRu(L)(η^2-C$_2$H$_4$)Ph Complexes

L	$\Delta G^{\ddagger}_{\text{insertion}}$
PMe$_3$	23.9
P(pyr)$_3$	23.2
P(OCH$_2$)$_3$CEt	20.1
P(OCH$_2$)$_2$(OCCH$_3$)	19.4
PF$_3$	18.3
CO	17.7

$\Delta\Delta G^{\ddagger}$ between the two processes is sufficiently small that ethylene C−H activation competes and only 20 TON of ethylbenzene is obtained before the catalyst is deactivated to form TpRu[P(OCH$_2$)$_3$CEt](η^3-C$_3$H$_4$Me). This suggests that k_{ins}/k_{act} is ~20 for TpRu[P(OCH$_2$)$_3$CEt](NCMe)Ph (k_{ins} is the rate constant for ethylene insertion, and k_{act} is the rate constant for ethylene C−H activation).[51] For **4**, k_{ins}/k_{act} is increased (to ~90) relative to the P(OCH$_2$)$_3$CEt complex, and multiple TON values of ethylbenzene production are observed. Thus, the modulation of $\Delta G^{\ddagger}$ for olefin insertion is a key factor in successful long-lived catalysis using TpRu(L)(NCMe)Ph complexes.

The TOF for catalytic hydrophenylation of ethylene by TpRu(L)(NCMe)Ph complexes also varies as a function of the identity of L, and a plot of TOF vs Ru(III/II) potential shows a good linear correlation (Figure 6). The TOFs were calculated

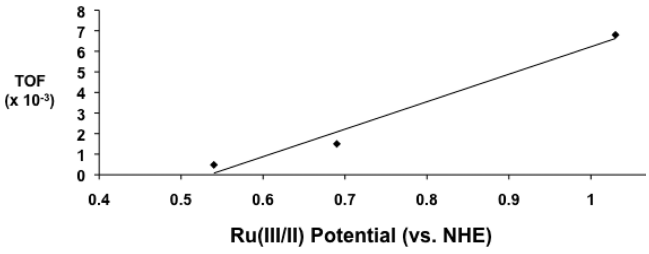

Figure 6. Plot of TOF vs Ru(III/II) potential for catalytic hydrophenylation of ethylene by TpRu(L)(NCMe)Ph (L = P(OCH$_2$)$_3$CEt, P(OCH$_2$)$_2$(OCCH$_3$), CO) using 0.025 mol % of catalyst and 15 psi of ethylene at 90 °C. The TOF was calculated after 4 h of reaction (R^2 = 0.97).

dx.doi.org/10.1021/om300676e | Organometallics 2012, 31, 6851−6860

Scheme 5. Calculated Gibbs Free Energies (kcal/mol) for Benzene C−H Activation and Formation of Ethylbenzene by TpRu(L)(η^2-C_2H_4)(CH_2CH_2Ph)

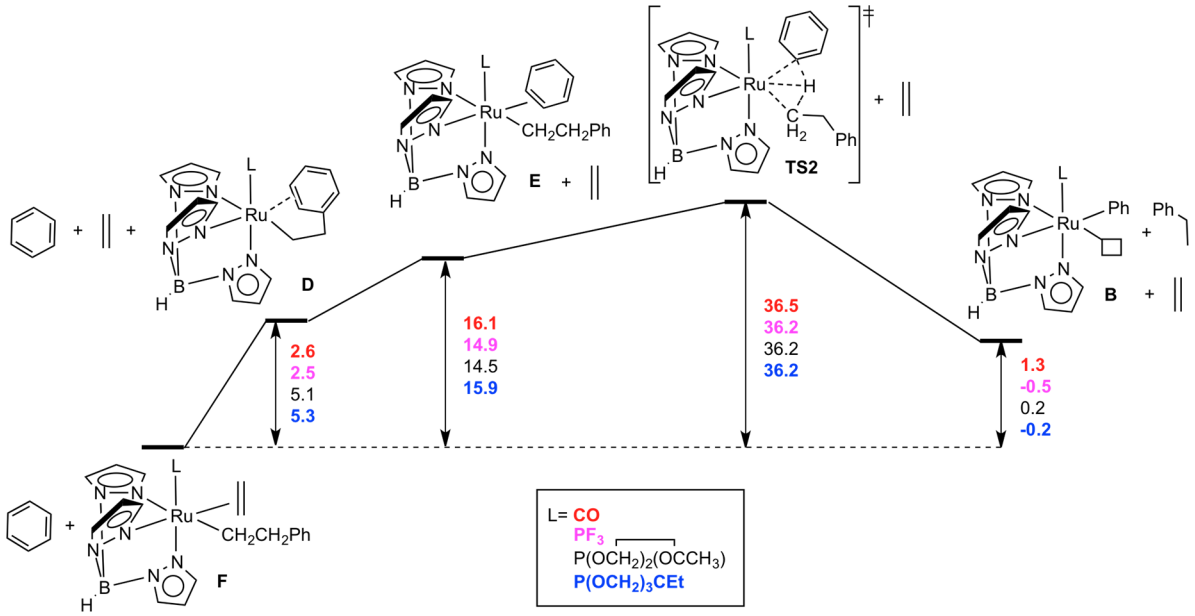

after 4 h, since there is no evidence of catalyst deactivation at this time point for any of the catalysts. Benzene C−H activation is the proposed rate-limiting step for the catalytic hydrophenylation of ethylene using TpRu(L)(NCMe)Ph complexes.[25] Thus, given the relative rates of C_6D_6 activation by TpRu(L)(NCMe)Ph complexes, which are opposite to the observed rates for catalytic ethylene hydrophenylation, the trend in TOF is more difficult to rationalize than TON. One potential explanation for the inverse trend for rates of stoichiometric benzene activation and TOF for catalytic hydrophenylation is that the rate of benzene C−H activation from proposed catalyst resting states, TpRu(L)(η^2-C_2H_4)(CH_2CH_2Ph), might be different from the observed relative rates of C_6D_6 activation by TpRu(L)(NCMe)Ph complexes. To probe this possibility, we calculated the energetics for benzene C−H activation starting from TpRu(L)(η^2-C_2H_4)(CH_2CH_2Ph) for the active catalysts L = CO, $P(OCH_2)_3CEt$, $P(\overline{OCH_2)_2(OCCH_3})$ (Scheme 5).

As Scheme 5 shows, within the anticipated error, the calculations predict identical activation barriers for the production of ethylbenzene from all of the TpRu(L)(η^2-C_2H_4)(CH_2CH_2Ph) complexes. Although these results do not reproduce the experimental observations, they are not surprising, given the small difference in activation barrier of ~2 kcal/mol between the most and least active catalysts. Perhaps most informative is a comparison of the ethylene binding energy among the series of TpRu(L)(η^2-C_2H_4)(CH_2CH_2Ph) complexes. Comparison of the energetics for ethylene dissociation from TpRu(L)(η^2-C_2H_4)(CH_2CH_2Ph) (**F**) to form TpRu(L)(κ^3-CH_2CH_2Ph) reveals that the phosphite complexes exhibit stronger binding energies of ethylene than the CO complex by 2.5 and 2.7 kcal/mol, respectively, for $P(\overline{OCH_2)_2(OCCH_3})$ and $P(OCH_2)_3CEt$. This could be a result of the more strongly donating character of the phosphite ligands in comparison to that of CO, which would enhance Ru to ethylene π back-bonding. The difference in binding energies might also be due to sterics; however, the calculated binding energy of ethylene for TpRu(PF_3)(η^2-C_2H_4)(CH_2CH_2Ph) is identical with that of the CO complex (given the expected error in calculations), which is consistent with the electronic effect playing a dominant role. We believe that more strongly donating ligands enhance ethylene binding for the proposed resting states TpRu(L)(η^2-C_2H_4)(CH_2CH_2Ph), which should increase the overall activation barriers for catalytic hydrophenylation of ethylene.

Summary and Conclusions. TpRu[$P(\overline{OCH_2)_2(OCCH_3})$](NCMe)Ph (**4**) has been shown to catalyze the hydrophenylation of ethylene to yield ~90 TO's of ethylbenzene after 50 h at 90 °C with 15 psi of ethylene. Complex **4** does not catalyze the hydrophenylation of propene or 1-pentene. A comparison of catalytic hydrophenylation of ethylene, or in some cases the failure of the complex to catalyze the reaction, by the series of TpRu(II) complexes TpRu(L)(NCMe)Ph (L = CO, PMe_3, $P(pyr)_3$, $P(OCH_2)_3CEt$, $P(\overline{OCH_2)_2(OCCH_3})$) allows some conclusions to be drawn.

(1) Increasing the donor ability of the ligand L of TpRu(L)(NCMe)Ph complexes increases the overall rate of stoichiometric benzene C−H activation.
(2) The influence of the donor ability of L on the rate of ethylene insertion into Ru−phenyl bonds appears to be the most important factor that determines the TON for Ru(II) catalysts.
(3) For TpRu(L)(NCMe)Ph catalysts, the steric profile of L plays an important role. For example, we have published data that suggest ethylene/NCMe exchange with TpRu[$P(pyr)_3$](NCMe)Ph is unfavorable due to sterics.[43]
(4) Although only three data points are available, the TOFs in Table 3 suggest that less electron-rich Ru(II) catalysts supported by poly(pyrazolyl) ligands are more active for ethylene hydrophenylation.

■ EXPERIMENTAL SECTION

General Methods. Unless otherwise noted, all synthetic procedures were performed under anaerobic conditions in a nitrogen-filled glovebox or by using standard Schlenk techniques. Glovebox purity was maintained by periodic nitrogen purges and was monitored by an oxygen analyzer

dx.doi.org/10.1021/om300676e | *Organometallics* 2012, 31, 6851−6860

(O_2(g) < 15 ppm for all reactions). Tetrahydrofuran was dried by distillation from sodium/benzophenone. Pentane was distilled over P_2O_5. Acetonitrile and diethyl ether were dried by distillation from CaH_2. Hexanes, benzene, and methylene chloride were purified by passage through a column of activated alumina. Benzene-d_6, acetonitrile-d_3, methylene chloride-d_2, and chloroform-d were stored under a nitrogen atmosphere over 4 Å molecular sieves. ^{1}H NMR spectra were recorded on a Varian Inova 500 MHz or Varian MRS 600 MHz spectrometer, and ^{13}C NMR spectra were recorded on a Varian Inova 500 MHz or Varian MRS 600 MHz spectrometer (operating frequency 126 or 151 MHz, respectively). All ^{1}H and ^{13}C NMR spectra are referenced against residual proton signals (^{1}H NMR) or the ^{13}C resonances of the deuterated solvent (^{13}C NMR). ^{31}P NMR spectra were obtained on a Varian Mercury Plus 300 MHz (operating frequency 121 MHz) spectrometer and referenced against an external standard of H_3PO_4 (δ 0). Resonances due to the Tp ligand in ^{1}H NMR spectra are listed by chemical shift and multiplicity only (all coupling constants for the Tp ligand are ~2 Hz).

Electrochemical experiments were performed under a nitrogen atmosphere using a BAS Epsilon potentiostat. Cyclic voltammograms were recorded in CH_3CN using a standard three-electrode cell from −1700 to +1700 mV at 100 mV/s with a glassy-carbon working electrode and tetrabutylammonium hexafluorophosphate as electrolyte. All potentials are reported versus NHE (normal hydrogen electrode) using ferrocene as the internal standard.

High-resolution electrospray ionization mass spectrometry (ESI-MS) analyses were obtained on a Bruker BioTOF-Q spectrometer at the University of Richmond. Samples were dissolved in acetonitrile and then mixed 3/1 with 0.1 M aqueous sodium trifluoroacetate (NaTFA) using $[Na(NaTFA)_x]^+$ clusters as an internal standard. These data are reported using the most intense peaks from the isotopic envelope for $[M + Na]^+$. The data are listed as m/z with the intensity relative to the most abundant peak of the isotopic envelope given in parentheses for both the calculated and observed peaks. The difference between calculated and observed peaks is reported in ppm. Low-resolution mass spectra were acquired on a Shimadzu G-17A/QP-5050 GC-MS instrument operating in EI-direct-inlet-MS mode. Mass spectra are reported as M^+ for originally neutral samples. In all cases, observed isotopic envelopes were consistent with the molecular composition reported.

The preparation, isolation, and characterization of TpRu[P(OCH$_2$)$_3$CEt](PPh$_3$)Cl,[42] TpRu(CO)Ph(NCMe),[35] TpRu[P(OCH$_2$)$_3$CEt]Ph(NCMe),[42] TpRu[P(pyr)$_3$]Ph(NCMe),[43] Ph$_2$Mg[THF]$_2$,[52] P(OCH$_2$)$_2$(OCCH$_3$),[48] and C(CH$_3$)(OH)(CH$_2$OH)$_2$[48] have been previously reported. P(OCH$_2$)$_3$CEt was obtained from a commercial source and purified by reconstitution in hexanes and filtration through Celite. The filtrate was concentrated to dryness to yield a white solid.

Calculations. Density functional theory calculations were performed using the Gaussian 09 suite of programs[53] employing the hybrid functional B3LYP with the effective core potential basis set CEP-31G(d).[42] Optimized geometries and transition states were confirmed by the presence of zero and one imaginary frequency, respectively, with thermochemistry determined at 298.15 K and 1 atm.

(η^6-*p*-cymene)Ru[P(OCH$_2$)$_2$(OCCH$_3$)]Br$_2$ (1). The complex [(η^6-*p*-cymene)Ru(Br)(μ-Br)]$_2$[55] (1.36 g, 1.73 mmol) was dissolved in 150 mL of methylene chloride and added to a round-bottom flask (500 mL) containing a benzene solution of P(OCH$_2$)$_2$(OCCH$_3$) (~1.13 g, 6.90 mmol, 200 mL of C_6H_6). The reaction mixture was stirred for 1 h and was then concentrated to ~20 mL under vacuum. Hexanes was added, and the mixture was stirred for 1 h. Hexanes was decanted through a fine-porosity frit with ~$^1/_3$ in. of Celite, and the filtrate was discarded. The Celite was washed with methylene chloride, and this second filtrate was placed back into the reaction flask. All solvent was removed under vacuum. The resulting solid was placed on a fine-porosity frit, washed with pentane, and dried in vacuo (1.67 g, 91% yield). ^{1}H NMR (600 MHz, $CDCl_3$): δ 5.74 (d, $^3J_{HH}$ = 6 Hz, 2H, *p*-cymene: C_6H_4), 5.61 (d, 2H, $^3J_{HH}$ = 6 Hz, *p*-cymene: C_6H_4), 4.21 (dt, 2H, $^2J_{HH}$ = 10 Hz, $^3J_{HP}$ = 5 Hz, P(OCH$_2$)$_2$(OCCH$_3$)), 3.86−3.82 (m, 2H, P(OCH$_2$)$_2$(OCCH$_3$)), 3.02 (sept, 1H, $^3J_{HH}$ = 7 Hz, *p*-cymene: C*H*(CH$_3$)$_2$), 2.36 (s, 3H, *p*-cymene: CH$_3$), 1.69 (s, 3H, P(OCH$_2$)$_2$(OCC*H*$_3$)), 1.26 (d, 6H, $^3J_{HH}$ = 7 Hz, *p*-cymene: CH(C*H*$_3$)$_2$). ^{13}C NMR (151 MHz, $CDCl_3$): δ 111.6, 106.4, 90.4, 90.3, 89.8, 89.8 (each a singlet, C_6H_4), 82.8 (s, P(OCH$_2$)$_2$(OCCH$_3$)), 75.86 (P(OCH$_2$)$_2$(OCCH$_3$)), 75.81 (P(OCH$_2$)$_2$(OCCH$_3$)), 31.2 (s, C_6H_4–*C*H(CH$_3$)$_2$), 22.4 (s, C_6H_4–CH(*C*H$_3$)$_2$), 15.3 (d, $^3J_{CP}$ = 11 Hz, P(OCH$_2$)$_2$(OC*C*H$_3$)). ^{31}P{^{1}H} NMR (121 MHz, $CDCl_3$): δ 140.5. HRMS: [M + Na$^+$] obsd (%), calcd (%), ppm: 548.85142 (20.2), 548.853 13 (23.7), −3.1; 549.852 63 (40.7), 549.853 55 (45.5), −1.7; 550.853 17 (57.1), 550.852 57 (64.7), 1.1; 551.853 22 (46.3), 551.852 51 (55), 1.3; 552.851 49 (100), 552.851 72 (100), −0.4; 553.851 81 (29.1), 553.852 52 (31.3), −1.3; 554.849 83 (49.9), 554.850 96 (70.3), −2.

(η^6-*p*-cymene)Ru[P(OCH$_2$)$_2$(OCCH$_3$)](Ph)Br (2). The complex (η^6-*p*-cymene)Ru[P(OCH$_2$)$_2$(OCCH$_3$)]Br$_2$ (**1**; 0.543 g, 1.10 mmol) in 75 mL of THF and Ph$_2$Mg[THF]$_2$ (0.331 g, 1.10 mmol) in 50 mL of THF were combined to give a red solution. Over a period of 45 min the red solution turned yellow with formation of a light pink precipitate. The mixture was filtered through Celite. The filtrate was concentrated to dryness, reconstituted in benzene, and filtered through Celite. The filtrate was loaded onto a $^1/_2$ in. plug of silica and washed with THF to elute a bright yellow band. The filtrate was reduced to ~10 mL, hexanes was added, and the mixture was reduced to dryness. The resulting yellow solid was collected, washed with pentane, and dried under vacuum (0.228 g, 42% yield). ^{1}H NMR (500 MHz, $CDCl_3$): δ 7.62 (dd, 2H, $^3J_{HH}$ = 8 Hz, $^4J_{HH}$ = 1 Hz, ortho phenyl), 6.98 − 6.85 (m, 3H, para and meta phenyl), 5.63 (dd, 1H, $^3J_{HH}$ = 6 Hz, $^4J_{HH}$ = 1 Hz, *p*-cymene: C_6H_4, fine coupling is observed for this resonance but other *p*-cymene resonances are too broad for resolution of fine coupling), 5.54 (d, 1H, $^3J_{HH}$ = 6 Hz, *p*-cymene: C_6H_4), 5.48 (d, 1H, $^3J_{HH}$ = 6 Hz, *p*-cymene: C_6H_4), 5.15 (d, $^3J_{HH}$ = 6 Hz, 1H, *p*-cymene: C_6H_4), 4.04 (td, $^2J_{HH}$ = 8 Hz, $^3J_{HP}$ = 4 Hz, 2H, P(OC*H*$_2$)$_2$(OCCH$_3$)), 3.70−3.61 (m, 2H, P(OC*H*$_2$)$_2$(OCCH$_3$)), 2.78 (sept, 1H, $^3J_{HH}$ = 7 Hz, *p*-cymene: C*H*(CH$_3$)$_2$), 1.89 (s, 3H, *p*-cymene: CH$_3$), 1.58 (s, 3H), 1.25 (d, 3H, $^3J_{HH}$ = 7 Hz, *p*-cymene: CH(C*H*$_3$)$_2$), 1.20 (d, 3H, $^3J_{HH}$ = 7 Hz, *p*-cymene: CH(C*H*$_3$)$_2$). ^{13}C NMR (126 MHz, $CDCl_3$): δ 151.3 (s, ipso of phenyl), 143.3, 126.9, 122.5 (each a singlet, phenyl), 118.4 (s, Cy-C_{quat}), 111.1 (s, *p*-cymene: C_{quat}), 95.0 (s, *p*-cymene: C_6H_4), 92.3 (d, $^2J_{PC}$ = 9 Hz, *p*-cymene: C_6H_4), 89.3, 89.1 (each a singlet, *p*-cymene: C_6H_4), 81.7 (P(OCH$_2$)$_2$(OCCH$_3$)), 75.4 (d, $^2J_{CP}$ = 2 Hz, P(OCH$_2$)$_2$(OCCH$_3$)), 75.3 (d, $^2J_{CP}$ = 2 Hz, P(OCH$_2$)$_2$(OCCH$_3$)), 31.4 (s, *p*-cymene: *C*H(CH$_3$)$_2$), 23.5 (s, *p*-cymene: CH(*C*H$_3$)$_2$), 22.2 (s, *p*-cymene: *C*H(CH$_3$)$_2$), 18.9 (s, *p*-cymene: CH$_3$), 15.35 (d, $^3J_{CP}$ = 10.7 Hz, P(OCH$_2$)$_2$(OC*C*H$_3$)). ^{31}P NMR (121 MHz, CD_2Cl_2): δ 155.5. HRMS: [M + Na$^+$] obsd (%), calcd (%), ppm: 546.974 55 (34.4), 546.974 31 (34.6), 0.4; 547.974 73 (65.1), 547.974 92 (66), 0.3; 548.9739 (100), 548.973 44 (100), 0.8; 549.974 59 (53.5), 549.972 93 (47.9), 3; 550.9734 (107.1), 550.972 94 (104.5), 0.8; 551.976 59 (85.5), 551.9763 (84.2), 0.5; 552.9734 (85.5), 552.971 81 (84.2), 2.9.

TpRu[P(OCH$_2$)$_2$(OCCH$_3$)](NCMe)Ph (4). The complex (η^6-*p*-cymene)Ru[P(OCH$_2$)$_2$(OCCH$_3$)](Ph)Br (**2**; 0.228 g, 0.434 mmol) was taken up in approximately 15 mL of NCMe, added to a pressure tube, and heated overnight at 75 °C. The reaction mixture was brought into the glovebox and cooled to room temperature. The mixture was filtered through Celite, and the filtrate was concentrated to dryness, yielding (NCMe)$_3$Ru[P(OCH$_2$)$_2$(OCCH$_3$)](Ph)Br (**3**). Without any purification, the resulting solid was taken up in ~10 mL of methylene chloride and added to a pressure tube along with a 5 mL solution of KTp (0.109 g, 0.434 mmol) in methylene chloride. The reaction was heated to 75 °C for 4 h. The reaction mixture was brought into the glovebox and filtered through Celite. The filtrate was concentrated to dryness and then reconstituted in diethyl ether (partially soluble). The mixture was loaded onto an 0.5 in. plug of silica and washed with 50 mL of diethyl ether. Methylene chloride (~100 mL) was used to elute a light yellow solution. The eluent was concentrated to ~5 mL and added to a stirred

dx.doi.org/10.1021/om300676e | *Organometallics* 2012, 31, 6851−6860

flask of hexanes. The mixture was concentrated to ~5 mL of solvent, and the resulting solid was collected on a fine-porosity frit. The solid was washed with pentane and dried in vacuo to yield an off-white solid (0.109 g, 44%). ^{1}H NMR (600 MHz, C_6D_6): δ 8.27, 8.00, 7.55, 7.38 (each a d, each 1H, Tp 3- and 5-positions), 7.70 (dd, 2H, $^3J_{HH}$ = 8 Hz, $^4J_{HH}$ = 1 Hz, ortho phenyl), 7.62 − 7.61 (m, 1H, Tp 3- or 5-position), 7.58, (s, 1H, Tp 3- or 5-position), 7.31 (t, 2H, $^3J_{HH}$ = 8 Hz, meta of phenyl), 7.20−7.16 (m, 2H, para phenyl), 6.20−6.17 (m, 1H, Tp 4-position), 6.03 (s, 1H, Tp 4-position), 5.96−5.95 (m, 1H, Tp 4-position), 3.41 (td, 2H, $^2J_{HH}$ = 7 Hz, $^2J_{HP}$ = 3 Hz, P(OCH_2)$_2$(OCCH$_3$)), 3.24 (dd, 1H, $^2J_{HH}$ = 7 Hz, $^3J_{HP}$ = 3 Hz), 3.17 (dd, 1H, $^2J_{HH}$ = 7 Hz, $^3J_{HP}$ = 3 Hz, P(OCH_2)$_2$(OCCH$_3$)), 0.82 (s, 3H, P(OCH_2)$_2$(OCCH$_3$)), 0.62 (s, 3H, CH_3CN). ^{13}C NMR (151 MHz, $CDCl_3$): δ 168.4 (d, $^2J_{CP}$ = 19 Hz, ipso phenyl), 146.7, 128.5, 124.7 (each a singlet, phenyl), 143.7, 142.4, 142.0, 135.1, 134.6, 133.8 (each a singlet, Tp 3- and 5-positions), 119.9 (N*C*CH$_3$), 105.2 (Tp 4-position), 104.9 (2C, overlapping Tp 4-position), 80.8 (P(OCH$_2$)$_2$(OCCH$_3$)), 74.6 (d, $^2J_{CP}$ = 2 Hz, P(OCH$_2$)$_2$(OCCH$_3$)), 74.5 (d, $^2J_{CP}$ = 2 Hz, P(OCH$_2$)$_2$(OCCH$_3$)), 15.6 (d, $^3J_{CP}$ = 10 Hz, P(OCH$_2$)$_2$(OC*C*H$_3$)), 4.5 (NC*C*H$_3$). ^{31}P NMR (121 MHz, $CDCl_3$, δ): 164.6. HRMS: [M + Na$^+$] obsd (%), calcd (%), ppm: 587.081 42 (42.6), 587.080 84 (44.6), 1; 588.079 74 (51.1), 588.080 42 (54.7), −1.2; 589.079 66 (73.8), 589.0809 (77.2), −2.1; 590.078 76 (100), 590.079 43 (100), −1.1; 591.081 34 (40.4), 591.082 28 (35.6), −1.6; 592.079 75 (63.8), 592.080 25 (54.6), −0.8; 593.080 74 (10.6), 593.082 69 (13.2), −3.3. Anal. Calcd for $C_{21}H_{25}BN_7O_3PRu$: C, 44.54; H, 4.45; N, 17.31. Found: C, 44.10; H, 4.52; N, 16.56. CV (NCMe): $E_{1/2}$ = 0.69 V Ru(III/II).

TpRu[P(OCH$_2$)$_2$(OCCH$_3$)](η^3-C$_3$H$_4$Me) (5). TpRu[P(OCH$_2$)$_2$(OCCH$_3$)](NCMe)Ph (**4**; 0.0384 g, 0.0678 mmol) was dissolved in 12 mL of benzene and placed in a stainless steel pressure reactor. The reactor was charged with 50 psi of ethylene and heated to 90 °C for 20 h. The volatiles were removed in vacuo. The residue was taken up in diethyl ether and loaded on a plug of silica gel and eluted with a 1/1 mixture of diethyl ether and pentane. The solvent was removed from the pale yellow filtrate in vacuo to give a beige solid (0.0162 g, 47% yield). ^{1}H NMR (600 MHz, C_6D_6): δ 8.23, 8.14, 7.73, 7.67, 7.55, 6.92 (each a d, each 1H, Tp 3- and 5-positions), 6.19, 6.11 (each a t, each 1H, Tp 4-position), 5.86 (s, 1H, Tp 4-position), 4.98 (m, 2H, H$_c$ in Chart 2), 3.27 (dd, 2H, $^3J_{HP}$ = 8 Hz, $^2J_{HH}$ = 6 Hz, P(OCH$_2$)$_2$(OCCH$_3$)), 3.17 (d, 1H, $^3J_{AC}$ = 7 Hz, H$_a$ in Chart 2), 3.04 (d, 2H, $^2J_{HH}$ = 6 Hz, 3H, P(OCH_2)$_2$(OCCH$_3$)), 2.48 (dq, 1H, $^3J_{DC}$ = 12 Hz, $^3J_{DMe}$ = 6 Hz, H$_d$ in Chart 2), 2.07 (d, 3H, $^3J_{MeD}$ = 6 Hz, CH_3 in Chart 2), 1.57 (d, 1H, $^3J_{AB}$ = 1 Hz, $^3J_{BC}$ = 11 Hz, H$_b$ in Chart 2), 0.81 (s, 3H, P(OCH$_2$)$_2$(OCCH_3)). ^{13}C NMR (151 MHz, C_6D_6): δ 147.0, 144.5, 138.4, 135.0, 134.8, 134.8 (each a singlet, Tp 3- and 5-positions), 105.5, 105.3, 105.1 (each a singlet, Tp 4-positions), 87.0 (allyl-CH$_2$*C*HCHCH$_3$), 80.3 (P(OCH$_2$)$_2$(OCCH$_3$)), 74.3 (d, $^2J_{CP}$ = 7 Hz, P(OCH$_2$)$_2$(OCCH$_3$)), 74.2 (d, $^2J_{CP}$ = 7 Hz, P(OCH$_2$)$_2$(OCCH$_3$)), 54.1 (d, $^2J_{CP}$ = 3 Hz, allyl-CH$_2$CH*C*HCH$_3$), 33.8 (d, $^2J_{CP}$ = 4 Hz, allyl-*C*H$_2$CHCHCH$_3$), 19.8 (s, allyl-CH$_2$CHCH*C*H$_3$), 14.7 (d, $^3J_{CP}$ = 10 Hz, P(OCH$_2$)$_2$(OC*C*H$_3$)). ^{31}P NMR (121 MHz, C_6D_6): δ 171.7. LRMS: obsd *m*/*z* (obsd %)/calcd %): 501 (42.6/45.5); 502 (53.6/54.5); 503 (71.9/77.5); 504 (100/100); 505 (33.8/32.1); 506 (58.5/55.0).

Chart 2. Allyl Coupling Diagram for TpRu[P(OCH$_2$)$_2$(OCCH$_3$)](η^3-C$_3$H$_4$Me) (5)

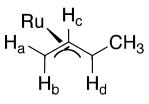

H–H Coupling	
$^2J_{ab}$	= 1 Hz
$^3J_{ac}$	= 7 Hz
$^3J_{bc}$	= 11 Hz
$^3J_{cd}$	= 12 Hz
$^3J_{dMe}$	= 6 Hz

Kinetic Studies: Rate Determination for Activation of C_6D_6 by TpRu[P(OCH$_2$)$_2$(OCCH$_3$)](NCMe)Ph (4). A solution of TpRu[P(OCH$_2$)$_2$(OCCH$_3$)](NCMe)Ph (**4**; 0.0115 g, 0.0203 mmol), acetonitrile (3.4 μL, 0.070 mmol), and a crystal of hexamethylbenzene (as an internal standard) in 2 mL of C_6D_6 (22.6 mmol) was equally divided and transferred into four J. Young NMR tubes. The solutions were heated to 60 °C in a temperature-regulated oil bath. ^{1}H NMR spectra were periodically acquired through 3 half-lives (using a pulse delay of 5 s). Relative to the internal standard hexamethylbenzene, the rates of Ru−Ph/Ru−Ph-d_5 exchange were followed by integration of the ortho phenyl resonance at 7.69 ppm.

Representative Catalytic Reaction. TpRu[P(OCH$_2$)$_2$(OCCH$_3$)](NCMe)Ph (**4**; 0.0048 g, 0.0085 mmol) was dissolved in 3 mL of benzene (with hexamethylbenzene as an internal standard). The homogeneous reaction mixture was transferred to a stainless steel pressure reactor that was charged with 15 psi of ethylene followed by pressurization with nitrogen to give a total pressure of 120 psi. The reactor was heated to 90 °C. After 2, 4, 6, 8, and 10 h, the reaction was analyzed by GC/MS using peak areas of the products and the internal standard to calculate product yields. Ethylbenzene production was quantified using linear regression analysis of gas chromatograms of standard samples. A set of five known standards were prepared consisting of 2/1, 3/1, 4/1, 5/1, and 6/1 molar ratios of ethylbenzene to hexamethylbenzene in methylene chloride. A plot of peak area ratios versus molar ratios gave a regression line. For the GC/MS system, the slope and correlation coefficient for ethylbenzene were 0.68 and 0.99, respectively.

■ ASSOCIATED CONTENT

Supporting Information

Figures, text, a table, and a CIF file giving representative NMR spectra, a discussion of calculated structures for **TS2** (Scheme 4), crystallographic data for complex **4**, data from mass spectrometry analysis, details of calculations, and full information for ref 53. This material is available free of charge via the Internet at http://pubs.acs.org.

■ AUTHOR INFORMATION

Corresponding Author

*E-mail: tbg7h@virginia.edu (T.B.G.); t@unt.edu (T.R.C.).

Notes

The authors declare no competing financial interest.

■ ACKNOWLEDGMENTS

We thank Dr. John G. Verkade of the Iowa State University Department of Chemistry for useful suggestions. We acknowledge the Office of Basic Energy Sciences, U.S. Department of Energy, for support of this work (DE-SC0000776 (T.B.G.) and DE-FG02-03ER15387 (T.R.C.)) and the National Science Foundation for financial support of instrumentation at the University of Richmond (CHE-0320669) and for the purchase of X-ray diffraction instrumentation at the University of Virginia (CHE-1126602).

■ REFERENCES

(1) Lewis, J. C.; Bergman, R. G.; Ellman, J. A. *Acc. Chem. Res.* **2008**, *41*, 1013−1025.
(2) Colby, D. A.; Bergman, R. G.; Ellman, J. A. *Chem. Rev.* **2010**, *110*, 624−655.
(3) Engle, K. M.; Mei, T.-S.; Wasa, M.; Yu, J.-Q. *Acc. Chem. Res.* **2012**, *45*, 788−802.
(4) Chen, X.; Engle, K. M.; Wang, D.-H.; Yu, J.-Q. *Angew. Chem., Int. Ed.* **2009**, *48*, 5094−5115.
(5) Neufeldt, S. R.; Sanford, M. S. *Acc. Chem. Res.* **2012**, *45*, 936−946.

(6) Daugulis, O.; Do, H.-Q.; Shabashov, D. *Acc. Chem. Res.* **2009**, *42*, 1074−1086.
(7) Hartwig, J. F. *Acc. Chem. Res.* **2011**, *45*, 864−873.
(8) Hickman, A. J.; Sanford, M. S. *ACS Catal.* **2011**, *1*, 170−174.
(9) Baxter, R. D.; Sale, D.; Engle, K. M.; Yu, J.-Q.; Blackmond, D. G. *J. Am. Chem. Soc.* **2012**, *134*, 4600−4606.
(10) Goj, L. A.; Gunnoe, T. B. *Curr. Org. Chem.* **2005**, *9*, 671−685.
(11) Ritleng, V.; Sirlin, C.; Pfeffer, M. *Chem. Rev.* **2002**, *102*, 1731−1769.
(12) Nadres, E. T.; Daugulis, O. *J. Am. Chem. Soc.* **2011**, *134*, 7−10.
(13) Andreatta, J. R.; McKeown, B. A.; Gunnoe, T. B. *J. Organomet. Chem.* **2011**, *696*, 305−315.
(14) Kakiuchi, F.; Kochi, T. *Synthesis-Stuttgart* **2008**, 3013−3039.
(15) Kubota, A.; Emmert, M. H.; Sanford, M. S. *Org. Lett.* **2012**, *14*, 1760−1763.
(16) Cucciolito, M. E.; D'Amora, A.; Tuzi, A.; Vitagliano, A. *Organometallics* **2007**, *26*, 5216−5223.
(17) Olah, G. A.; Molnar, A. *Hydrocarbon Chemistry*, 2nd ed.; Wiley-Interscience: New York, 2003.
(18) Roberts, R. M.; Khalaf, A. A. *Friedel-Crafts Alkylation Chemistry: A Century of Discovery*; Marcel Dekker: New York, 1984.
(19) Perego, C.; Ingallina, P. *Green Chem.* **2004**, *6*, 274−279.
(20) Kocal, J. A.; Vora, B. V.; Imai, T. *Appl. Catal., A* **2001**, *221*, 295−301.
(21) Perego, C.; Ingallina, P. *Catal. Today* **2002**, *73*, 3−22.
(22) Degnan, T. F.; Smith, C. M.; Venkat, C. R. *Appl. Catal., A* **2001**, *221*, 283−294.
(23) Corma, A.; Garcia, H. *Chem. Rev.* **2003**, *103*, 4307−4365.
(24) Cejka, J.; Wichterlova, B. *Catal. Rev.* **2002**, 375−421.
(25) Foley, N. A.; Lee, J. P.; Ke, Z. F.; Gunnoe, T. B.; Cundari, T. R. *Acc. Chem. Res.* **2009**, *42*, 585−597.
(26) Oxgaard, J.; Muller, R. P.; Goddard, W. A.; Periana, R. A. *J. Am. Chem. Soc.* **2004**, *126*, 352−363.
(27) Jia, C.; Piao, D.; Oyamada, J.; Lu, W.; Kitamura, T.; Fujiwara, Y. *Science* **2000**, *287*, 1992−1995.
(28) Bowring, M. A.; Bergman, R. G.; Tilley, T. D. *Organometallics* **2011**, *30*, 1295−1298.
(29) Jia, C. G.; Kitamura, T.; Fujiwara, Y. *Acc. Chem. Res.* **2001**, *34*, 633−639.
(30) Kakiuchi, F.; Murai, S. *Acc. Chem. Res.* **2002**, *35*, 826−834.
(31) Colby, D. A.; Bergman, R. G.; Ellman, J. A. *Chem. Rev.* **2010**, *110*, 624−655.
(32) Luedtke, A. T.; Goldberg, K. I. *Angew. Chem., Int. Ed.* **2008**, *47*, 7694−7696.
(33) Periana, R. A.; Liu, X. Y.; Bhalla, G. *Chem. Commun.* **2002**, 3000−3001.
(34) McKeown, B. A.; Foley, N. A.; Lee, J. P.; Gunnoe, T. B. *Organometallics* **2008**, *27*, 4031−4033.
(35) Lail, M.; Bell, C. M.; Conner, D.; Cundari, T. R.; Gunnoe, T. B.; Petersen, J. L. *Organometallics* **2004**, *23*, 5007−5020.
(36) Karshtedt, D.; Bell, A. T.; Tilley, T. D. *Organometallics* **2004**, *23*, 4169−4171.
(37) Oxgaard, J.; Periana, R. A.; Goddard, W. A. *J. Am. Chem. Soc.* **2004**, *126*, 11658−11665.
(38) McKeown, B. A.; Gonzalez, H. E.; Friedfeld, M. R.; Gunnoe, T. B.; Cundari, T. R.; Sabat, M. *J. Am. Chem. Soc.* **2011**, *133*, 19131−19152.
(39) Karshtedt, D.; McBee, J. L.; Bell, A. T.; Tilley, T. D. *Organometallics* **2006**, *25*, 1801−1811.
(40) Oxgaard, J.; Goddard, W. A. *J. Am. Chem. Soc.* **2004**, *126*, 442−443.
(41) Jones, W. D.; Maguire, J. A.; Rosini, G. P. *Inorg. Chim. Acta* **1998**, *270*, 77−86.
(42) Foley, N. A.; Ke, Z. F.; Gunnoe, T. B.; Cundari, T. R.; Petersen, J. L. *Organometallics* **2008**, *27*, 3007−3017.
(43) Foley, N. A.; Lail, M.; Gunnoe, T. B.; Cundari, T. R.; Boyle, P. D.; Petersen, J. L. *Organometallics* **2007**, *26*, 5507−5516.
(44) Foley, N. A.; Lail, M.; Lee, J. P.; Gunnoe, T. B.; Cundari, T. R.; Petersen, J. L. *J. Am. Chem. Soc.* **2007**, *129*, 6765−6781.
(45) Lail, M.; Arrowood, B. N.; Gunnoe, T. B. *J. Am. Chem. Soc.* **2003**, *125*, 7506−7507.
(46) Pittard, K. A.; Cundari, T. R.; Gunnoe, T. B.; Day, C. S.; Petersen, J. L. *Organometallics* **2005**, *24*, 5015−5024.
(47) Foley, N. A.; Gunnoe, T. B.; Cundari, T. R.; Boyle, P. D.; Petersen, J. L. *Angew. Chem., Int. Ed.* **2008**, *47*, 726−730.
(48) Joslin, E. E.; McMullin, C. L.; Gunnoe, T. B.; Cundari, T. R.; Sabat, M.; Myers, W. H. *Inorg. Chem.* **2012**, *51*, 4791−4801.
(49) Disappearance of the coordinated *p*-cymene resonances and appearance of free *p*-cymene resonances are observed by ^{1}H NMR spectroscopy for reaction of **2** in $NCCD_3$.
(50) The percent yield was determined by ^{1}H NMR spectroscopy using an internal standard.
(51) Since ethylene C−H activation irreversibly deactivates the catalyst, the ratio of k_{ins} and k_{act} was estimated from the TON for each catalyst.
(52) Lühder, K.; Nehls, D.; Madeja, K. *J. Prakt. Chem.* **1983**, *325*, 1027−1029.
(53) Frisch, M. J., et al. *Gaussian 09*; Gaussian, Inc: Wallingford, CT, 2009.
(54) Stevens, W. J.; Krauss, M.; Basch, H.; Jasien, P. G. *Can. J. Chem.* **1992**, *70*, 612−630.
(55) Mendoza-Ferri, M. G.; Hartinger, C. G.; Nazarov, A. A.; Eichinger, R. E.; Jakupec, M. A.; Severin, K.; Keppler, B. K. *Organometallics* **2009**, *28*, 6260−6265.